Realistic Representation of Middle-mass White Dwarfs

and Collisions with Black Holes

Mitchell Lachat

Advisor: Dr. James Lombardi, Jr.
Second Reader: Dr. Daniel Willey

ALLEGHENY COLLEGE

PHYSICS

Deparment of Physics
Allegheny College
Meadville, Pennsylvania
April 2020

Abstract

White Dwarfs are compact objects that have been observed for over one hundred years. They are a very common step in the evolution of stars. Because of how common these objects are, we expect them to collide with other stars. We begin out study of white dwarfs by using the smoothed particle hydrodynamics code *StarSmasher* to collide two $n = 1.5$ polytropes. These types of polytropes are shown to be a good approximation from low mass white dwarfs. To study white dwarfs of higher masses, we need to implement electron degeneracy pressure. We use zero-temperature electron degeneracy pressure to model more realistic white dwarfs of higher masses. For our initial study, we simulated a white dwarf with a mass of 0.51 $M_\odot$. As a proof of concept for this new way to calculate pressure, we collided two of these white dwarfs together to make sure that the code was stable. From there, we tried colliding them with black holes that were represented by point particles with mixed results. Just after the first pass, particles were falling onto the black hole and the code would terminate without continuing any farther. We are currently looking into the cause of the stoppage and plan to create a more complex equation for pressure that takes into account more than just zero-temperature electron degeneracy pressure.

Acknowledgements

I want to thank the following people:

Dr. Lombardi: For his unwavering support in my journey through physics. He was always there when I needed him to be yet pushed me to grow as a physicist and as a person. He was never afraid to check in to see how I as doing. Without him, I would not be the person I am today.

Dr. Poynor: For her no-nonsense attitude. At first, she seemed intimidating, but in reality she is one of the most approachable people that I have ever met. I know that if I want talk about anything, she is always in the lounge and ready to chat.

Alex Urban: For his welcome opinions. Ten years ago, he was in a similar position as I was. Having been through it recently, I looked to him for the more personal guidance. he also opened my eyes to some of the pitfalls of graduate school. He also puts mental health first. Something that I had heard before but had never been so fervently supported. He has taught me more things than I thought in the one year that he was with us.

Dr. Statman: For his teaching of complicated topics. I took arguably the hardest physics class in my sophomore year. He broke everything down and gave us plenty of opportunities to figure out the material ourselves as that is the only way to truly understand this material.

Dr. Rahman: For his eloquence and his focus on the details. The things that you have taught me are the following: efficiency is important but nothing is more important than love. I am glad to have been here while you taught your final classes.

Dr. Willey: For his ability to share the world of physics with many people. I did not have any classes with you but many of my friends did. You were able to make people think about the introductory material in a way that is enjoyable.

Dr. Petasis: For his willingness to push me intellectually. The largest step in the curriculum for physics major is Modern Physics. It was stressful but it gave me invaluable problem solving skills.

Physics Fam: For the memorable moments. I had so much fun hanging out with everyone. You were invaluable in your support. We did so many things together, and I will miss you guys the most. Special thanks goes to Travis Court for making me a member of the Physics Fam before I became a student.

Betsy and Everyone in Ballroom: For your friendship. Betsy is more of a friend than a professor to me. Ballroom was a way for me to de-stress, and it was some of the most fun that I have had my whole time at Allegheny College.

Dr. Niblock, Carol, Vicky, Ward, and the Choirs: For the music that we made together. I will never forget the amount of memories that we had singing in the choir room or the stairwell. Even in opera scenes, without a performance, I had some of my favorite experiences.

Contents

List of Figures

Chapter 1

Introduction

There are a countless number of objects in the universe. Due to gravity, matter clumps together and objects collide. Some of these collisions are between two compact objects. LIGO (Laser Interferometer Gravitational-Wave Observatory) has recorded data on binary black hole mergers as well as binary neutron star mergers [1–8]. In LIGO's third observing window, they hope to capture data on collisions between neutron stars and black holes. There is growing excitement for even more data on events involving black holes and neutron stars. However, black holes and neutron stars are not the only things classified as compact objects.

White dwarfs are thought to collide with other compact objects in star clusters such as M15 [9]. Within these clusters, they would collide with stellar mass black holes of around $10\,M_\odot$ just as other objects have been predicted [10]. Thus we will be taking a look at collisions between white dwarfs and black holes using the smoothed particles hydrodynamics code *Starsmasher*.

Chapter 2

Theory

2.1 Newtonian Gravity

Isaac Newton (1642-1727) was born on Christmas Day in 1642 which was also the same year as the death of another notable physicist, Galileo Galilei (1564-1642). Newton received his bachelor's degree from Cambridge University. Two years later while living at home in Woolsthorpe, England, Newton made many discoveries and advances in the understanding of motion, astronomy, mathematics, and optics. He did not publish his finding immediately but in 1687, he released the *Philosophia Naturalis Principia Mathematica*, or the *Mathematical Principles of Natural Philosophy*, which is simply referred to as the *Principia*. The *Principia* contained many of Newton's findings including mechanics, gravitation, and calculus [11].

2.1.1 Newton's Law's of Motion

Everyone has experienced gravity in some way. The closer that something is to an object, such as Earth, the larger the force of gravity. Likewise, the farther away an object is, the smaller the force that they experience. The force of gravity is symmetric. Therefore the force of gravity experienced by the Earth is the same force experienced by the Sun. To view this mathematically, we will begin with Newton's Second Law which states that the net force on

an object experiencing n forces is

$$\mathbf{F}_{\text{net}} = \sum_{i=1}^{n} \mathbf{F}_i = m\mathbf{a} \tag{2.1}$$

where $\mathbf{F}_{net}$ is the total force applied to the object, $\mathbf{F}_i$ is the ith force applied to the object, m is the mass of the object experiencing the force, and $\mathbf{a}$ is the acceleration of the object experiencing the force [11].[1]

Equation 2.1 is seen in all introductory physics courses. However, it assumes that the mass of object remains constant. This is not necessarily true. Consider a rocket moving in open space. As it burns fuel to move forward, it is losing mass in the process. Therefore, a more general statement of Newton's second law is

$$\mathbf{F}_{\text{net}} = \frac{d\mathbf{p}}{dt} \tag{2.2}$$

where $\mathbf{F}_{net}$ is the total force applied to the object and $\frac{d\mathbf{p}}{dt}$ is the rate of change in the momentum. Notice that if the mass is constant, Equation 2.2 reduces to Equation 2.1 since

$$\frac{d\mathbf{p}}{dt} = \frac{d(m\mathbf{v})}{dt} = m\frac{d\mathbf{v}}{dt} = m\mathbf{a}$$

where $\frac{d\mathbf{v}}{dt}$ is the reate of change in the velocity [11].

Newton's third law states that for every force, there is another force equal in magnitude but opposite in direction. This means that

$$\mathbf{F}_{12} = -\mathbf{F}_{21} \tag{2.3}$$

where $\mathbf{F}_{12}$ is the force of object 1 on object 2 and $\mathbf{F}_{21}$ is the force of object 2 on object 1. With Equation 2.3, only one of the forces must be represented. The other force is implied

[1] Hereafter, all variables in bold are vectors with a magnitude and direction. If variables are not bold, they are only magnitudes.

to exist [11].

2.1.2 Universal Law of Gravitation

Isaac Newton, by observing the movement of the planets, determined that the force of gravity applied to all objects was not the same. He found that the force of gravity depended on the mass of nearby objects as well as the distance to them. Thus he found the following relationship:

$$\mathbf{F}_{grav} = -\frac{GMm}{r^2}\hat{\mathbf{r}} \tag{2.4}$$

where $\mathbf{F}_{grav}$ is the force of gravity experienced by an object due to another object, G is the universal gravitational constant,[2] M is the mass of the object exhibiting the force, m is the mass of the object experiencing the force, r is the distance between the two objects, and $\hat{\mathbf{r}}$ is a unit vector along the line between the two objects that points away from the source of the gravitational force. Note that in Equation 2.4, the force is in the negative $-\hat{\mathbf{r}}$ direction. Physically, this means that gravity is an attractive force [11].

2.1.3 Work and Energy

Energy plays an important role in astrophysical systems. We can use it to determine whether object are gravitationally bound or to determine properties such as temperature. In this case, we look at the internal, kinetic, and gravitational potential energy of objects in our system. To find the gravitational potential energy of the system, we can use the work-energy theorem which states that

$$U_f - U_i = \Delta U = -\int_{\mathbf{r}_i}^{\mathbf{r}_f} \mathbf{F} \cdot d\mathbf{r} \tag{2.5}$$

where U is the potential energy, $\mathbf{r}$ is the position vector, and $d\mathbf{r}$ is the infinitesimal change in the position vector.[3] By applying Equation 2.4 to Equation 2.5, our integral involving

[2] See Appendix B for the value of all constants used in this paper.

[3] The subscripts in this equation represent initial and final states. So U_f and U_i are the final and initial potential energies.

potential energy becomes

$$\Delta U = \int_{r_i}^{r_f} \frac{GMm}{r^2}\, dr.$$

Therefore, we have

$$U_f - U_i = -GMm\left(\frac{1}{r_f} - \frac{1}{r_i}\right).$$

Because we can choose any reference point for zero potential energy, we can set U_i to be zero as $r_i \to \infty$ and $r_f = r$. Thus the potential energy is

$$U = -\frac{GMm}{r}. \tag{2.6}$$

Note that based on our reference point, gravitational potential energy is always negative [11].

For an object of mass m to escape the gravitational influence of a body of mass M, it must have sufficient kinetic energy. The least amount of energy needed to achieve this would be when the the total mechanical energy of the system is zero. When this occurs, our object will be at $r = \infty$ with no velocity so there will be no kinetic energy. Therefore

$$E = T + U = \frac{1}{2}mv_{\text{esc}}^2 - \frac{GMm}{r} = 0$$

where T is the kinetic energy of the object. If we solve this equation for v_{esc}, we find the escape velocity for an object:

$$v_{\text{esc}} = \sqrt{\frac{2GM}{r}}. \tag{2.7}$$

Notice that escape velocity is not dependent on the mass of the moving body [11].

Work also plays an important role in the thermodynamic properties of a gas. This is illustrated in the first law of thermodynamics

$$dE_{\text{int}} = -P\, dV, \tag{2.8}$$

where E_{int} is the internal energy, P is the pressure, and V is the volume. Notice that there is no heat dependence in Equation 2.8. So to find the internal energy we need to take an integral. However, before we do that, it will be helpful to express Equation 2.8 in terms of density instead of volume. Therefore, Equation 2.8 becomes

$$dE_{\text{int}} = -P\,d\left(\frac{m}{\rho}\right) = -Pm\,d\left(\frac{1}{\rho}\right) = -\frac{Pm}{\rho^2}\,d\rho.$$

Therefore the internal energy can be expressed in the following way:

$$u = \frac{E_{\text{int}}}{m} = -\int \frac{P}{\rho^2}\,d\rho. \tag{2.9}$$

We will now be referring to u as the specific internal energy.

2.2 Polytropes

The universe is complicated. Because of this, there are many approximations that are made to simulate it. For stars, the most common approximation are polytropes. Polytropes are stars defined to have the following properties:

1. The relation between pressure and density is $P \sim \rho^{\gamma}$ for some constant γ.
2. The star solves the equation of hydrostatic equilibrium with spherical symmetry. [4]

The simplest way to formulate a relation between pressure and density is $P \sim \rho^{\gamma}$. Every star can be approximated by using a particular value of γ. It is common practice to let γ be $1 + \frac{1}{n}$ where n is the polytropic index. In this case, we can relate pressure and density in the following way:

$$P = K\rho^{1+\frac{1}{n}} \tag{2.10}$$

where P is pressure, K is a constant, ρ is density, and n is the polytropic index. It has been

[4] We will break down the equation of hydrostatic equilibrium in Section 2.2.1

seen that white dwarfs are most accurately represented with a polytropic index of $n = 1.5$ in the low mass regime and $n = 3$ for the high mass regime [11, 12].[5]

2.2.1 Hydrostatic Equilibrium

Now that we have an expression for the pressure within a polytrope, we need to know how a polytrope uses pressure to support itself. The pressure given in Equation 2.10 must be balanced by the gravitation attraction of every particle within the star. This interaction can be described by using the equation for hydrostatic equilibrium

$$\frac{dP}{dr} = -g(r)\rho(r), \tag{2.11}$$

where P is pressure, r is the radius from the center of the star, g is the local gravitational acceleration at a certain radius r, ρ is the density of the star at r. Note that due to the radial symmetry of stars, all of the quantities in Equation 2.11 are only dependent on the distance to the center [11].

2.2.2 Lane-Emden Equation

Equation 2.10 relates the pressure and density within a polytrope. Now we need to relate density with radius. To do this, we must solve the Lane-Emden equation. We begin with the equation for hydrostatic equilibrium, Equation 2.11. By using Equation 2.4, we can rewrite Equation 2.11 as

$$\frac{dP}{dr} = -\frac{GM_r}{r^2}\rho$$

where M_r is the total mass inside a sphere of radius r [11].

Then we can rearrange and take the radial derivative of each side to receive

$$\frac{d}{dr}\left(\frac{r^2}{\rho}\frac{dP}{dr}\right) = -G\frac{dM_r}{dr}$$

[5] We will prove this in Section 2.3.1

which by using the fact that

$$\frac{dM_r}{dr} = 4\pi r^2 \rho$$

we have

$$\frac{d}{dr}\left(\frac{r^2}{\rho}\frac{dP}{dr}\right) = -G(4\pi r^2 \rho)$$

or

$$\frac{1}{r^2}\frac{d}{dr}\left(\frac{r^2}{\rho}\frac{dP}{dr}\right) = -4\pi G\rho. \tag{2.12}$$

To proceed, we must now invoke Equation 2.10. By using Equation 2.10 as our pressure equation for Equation 2.12, we can take the appropriate derivatives and simplify to receive

$$\left(\frac{n+1}{n}\right)\frac{K}{r^2}\frac{d}{dr}\left[r^2\rho^{(1-n)/n}\frac{d\rho}{dr}\right] = -4\pi G\rho.$$

To simplify the last equation, it is helpful to rewrite it in a dimensionless form. We can represent the density in terms of the central density ρ_c and a dimensionless function of r which we will denote as θ. So let

$$\rho(r) \equiv \rho_c[\theta_n(r)]^n, \text{ where } 0 \leq \theta_n \leq 1. \tag{2.13}$$

By substituting and simplifying, we arrive at

$$\left[(n+1)\left(\frac{K\rho_c^{(1-n)/n}}{4\pi G}\right)\right]\frac{1}{r^2}\frac{d}{dr}\left[r^2\frac{d\theta_n}{dr}\right] = -\theta_n^n.$$

This is the most general form of the Lane-Emden Equation. It is usually not expressed this way [11].

Notice that the leftmost expression in brackets is a constant with units of distance

squared. Therefore, by defining

$$\lambda_n \equiv \left[(n+1) \left(\frac{K \rho_c^{(1-n)/n}}{4\pi G} \right) \right]^{1/2} \tag{2.14}$$

and introducing the dimensionless independent variable ξ via

$$r \equiv \lambda_n \xi,$$

we finally obtain the Lane-Emden equation

$$\frac{1}{\xi^2} \frac{d}{d\xi} \left[\xi^2 \frac{d\theta_n}{d\xi} \right] = -\theta_n^n. \tag{2.15}$$

Solving the Lane-Emden equation, Equation 2.15, for the function $\theta_n(\xi)$ in terms of ξ for a particular value of the polytropic index n directly gives the density profile in terms of radius $\rho_n(r)$. Using this solution and the equation for hydrostatic equilibrium, Equation 2.11, we have our polytrope [11].

2.3 White Dwarfs

White Dwarfs are the last stage of stellar evolution for some stars. They are formed from the death of stars less than about $8\,M_\odot$ [14]. White dwarfs are the remaining core from stars that are no longer hot enough to be powered through fusion. The composition of these remnants are dependent on the initial mass of the progenitor. Low mass stars result in white dwarfs composed mostly of carbon while stars closer to $8\,M_\odot$ result in white dwarfs made up of heavier elements such as oxygen and neon [14]. Regardless of composition, white dwarf are supported by electron degeneracy pressure. We will approximate that the white dwarf has a temperature of $0\,K$. Such an approximation is reasonable because the primary support structure of white dwarfs is electron degeneracy pressure. It dominates the pressure

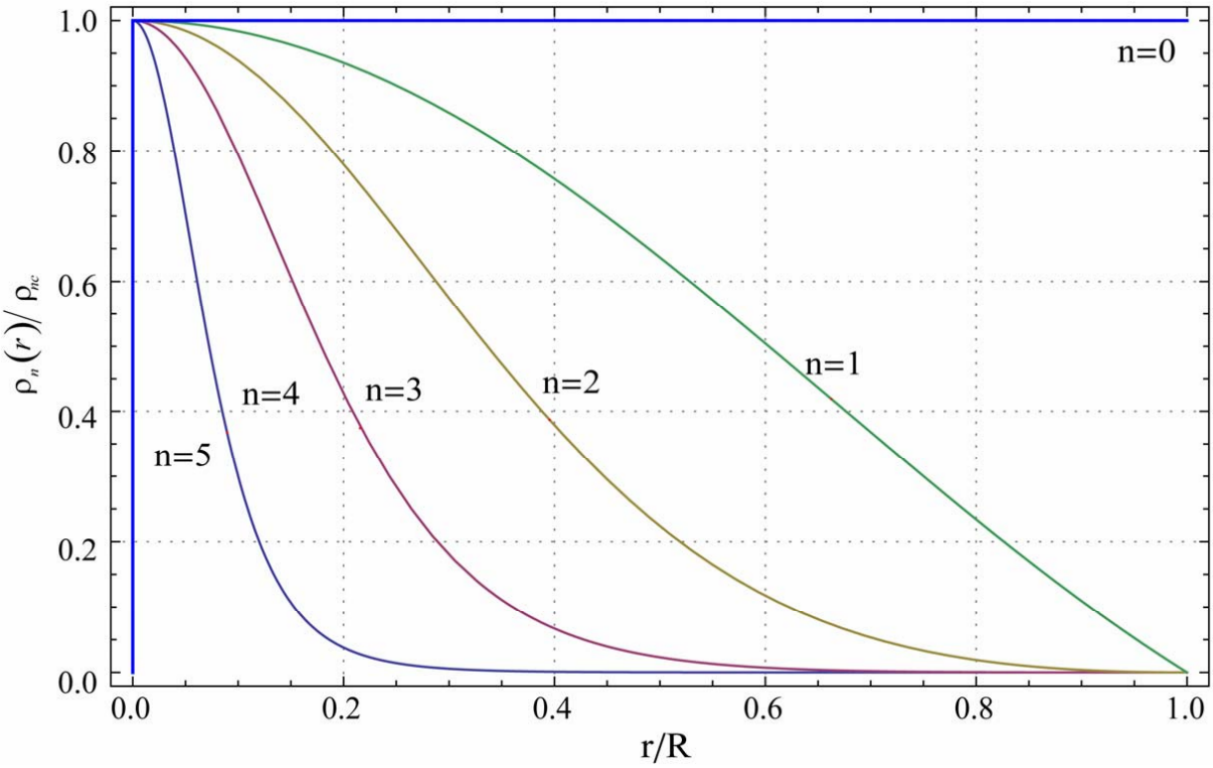

Figure 2.1: Graph showing the normalized mass density profiles as a function of fractional radius for polytropes. The $n = 5$ line should continue horizontally along the horizontal axis at a value of 0. The $n = 5$ polytrope is centrally concentrated at a finite radius but the entire polytrope has a radius that extends to infinity. The $n = 0$ polytrope has a uniform density throughout the star [13]

.

experienced within white dwarfs so this makes sense as an approximation.

2.3.1 Electron Degeneracy Pressure

Electron degeneracy pressure is a direct result of the Pauli exclusion principle. The Pauli exclusion principle states that a fermion cannot be in the same quantum state as another fermion. In the case of white dwarfs, atoms are so close together that electrons are not associated with any particular nuclei. Therefore, the electrons are considered free electrons. Now, we can apply the Heisenberg uncertainty principle to show that there is pressure that exists due to these free electrons [15–17].

The Heisenberg uncertainty principle states

$$\sigma_x \sigma_p \geq \frac{h}{4\pi}$$

where σ_x is the uncertainty in the position of the particles, σ_p is the uncertainty in the momentum of the particles, and h is the Planck constant. Therefore as particles get closer and closer together, the uncertainty in their position decreases which results in an increase in uncertainty of the momentum. Therefore, there must be a wide range of momenta in that space and this creates a pressure. To quantify this pressure, we must understand the Fermi sphere [17].

If we plot the momenta of all the particles in a white dwarf, we would see a sphere that forms as shown in Figure 2.2. This is because we are assuming that the gas is at 0 K so all of the particles want to be in the ground state. The largest momenta in magnitude is the Fermi momentum which is the radius of the Fermi sphere. We can say that the minimum number of electrons that fit inside the Fermi sphere is

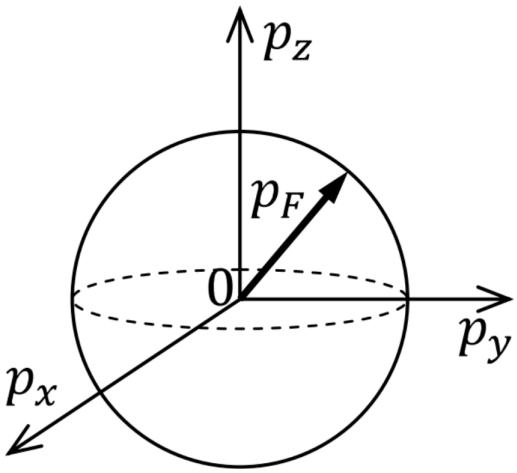

Figure 2.2: Graphical representation of Fermi sphere where is largest momentum in magnitude is the Fermi momentum. Image from the University of Frankfurt.

$$n_{\mathrm{e}} = \frac{8\pi}{3h^3} p_{\mathrm{f}}^3$$

which is received from an analysis of the density of particles in the momentum phase space. By solving for the Fermi momentum and relating the number of electrons to a density, we have

$$p_{\mathrm{f}} = \left(\frac{3h^3}{8\pi} \cdot \frac{\rho}{\mu_{\mathrm{e}} m_{\mathrm{H}}} \right)^{1/3} \tag{2.16}$$

where ρ is the density of the gas, $\mu_{\rm e}$ is the number of nucleons per electron in each atom, and m_H is the mass of a hydrogen atom [15].

Due to the high density of particles within a white dwarf, we expect the mean free path for electrons to be small. Therefore, it follows from diffusion that the number of electrons that cross an area in a certain time from both sides is given as

$$F \approx \frac{1}{3} n_{\rm e} v$$

where v is the velocity of the electrons. Thus the pressure at the boundary where electrons have momentum p and a velocity v is

$$P = \frac{1}{3} n_{\rm e}(v) v p.$$

Then the total pressure is given by

$$P_{\rm tot} = \frac{1}{3} \int_0^\infty n_{\rm e}(v) v p \, dv = \frac{1}{3} \int_0^\infty n_{\rm e}(p) v p \, dp \text{ [15].} \tag{2.17}$$

Within a white dwarf, there may be electrons that have enough energy to be relativistic so we will define

$$p = \frac{m_{\rm e} c}{\sqrt{1 - v^2/c^2}}. \tag{2.18}$$

By combining Equation 2.17 and Equation 2.18, we find that the pressure due to degenerate electrons is given by

$$P_{\rm e} = \frac{1}{3} \int_0^{p_{\rm f}} \frac{8\pi p^3}{h^3} \left(\frac{p/m_{\rm e}}{\sqrt{1 + p^2/(m_{\rm e}^2 c^2)}} \right) dp.$$

Notice that because $T = 0$ the integral over all space is the same as the integral over the Fermi sphere. If we let $\zeta = p/(m_{\rm e} c)$ and $x = p_{\rm f}/(m_{\rm e} c)$, our integral becomes

$$P_{\rm e} = \frac{8\pi m_{\rm e}^4 c^5}{3h^3} \int_0^x \frac{\zeta^4}{\sqrt{1 + \zeta^2}} \, d\zeta.$$

Computing, the integral, we find that

$$\int_0^x \frac{\zeta^4}{\sqrt{1+\zeta^2}}\,d\zeta = \frac{1}{8}x(2x^2-3)(1+x^2)^{1/2} + \frac{3}{8}\sinh^{-1}x.$$

By defining

$$f(x) = x(2x^2-3)(1+x^2)^{1/2} + 3\sinh^{-1}x, \tag{2.19}$$

the pressure due to degenerate electrons is given by

$$P_\mathrm{e} = \frac{\pi m_\mathrm{e}^4 c^5}{3h^3} f(x)\ [15]. \tag{2.20}$$

Let's consider a few limiting cases. First, assume that the Fermi momentum is much less than $m_\mathrm{e}c$, or that $p_\mathrm{f} \ll m_\mathrm{e}c$. In other words, the electrons are non-relativistic. This means that $x \ll 1$ because $x = p_\mathrm{f}/(m_\mathrm{e}c)$. Because x is small, we can find the Taylor expansion of $f(x)$. For small x,

$$f(x) \approx \frac{8}{5}x^5 - \frac{4}{7}x^7 + \frac{1}{3}x^9 + O(x^{11})$$

where $O(x^{11})$ represents the terms of order x^{11} and higher. By only taking the dominant term and substituting for x, we find that

$$P_\mathrm{e} = \frac{\pi m_\mathrm{e}^4 c^5}{3h^3}\frac{8}{5}x^5 = \frac{8\pi m_\mathrm{e}^4 c^5}{15h^3}\left(\frac{p_\mathrm{f}}{m_\mathrm{e}c}\right)^5 = \frac{8\pi}{15h^3 m_\mathrm{e}}p_\mathrm{f}^5.$$

Now by using Equation 2.16, the pressure due to degenerate electrons at small values of x is

$$P_\mathrm{e} = \frac{h^2}{20\,m_\mathrm{e}}\left(\frac{3}{\pi}\right)^{2/3}\left(\frac{\rho}{\mu_\mathrm{e}m_\mathrm{H}}\right)^{5/3}. \tag{2.21}$$

Therefore $P_\mathrm{e} \sim \rho^{5/3}$. If we let $\gamma = 5/3$ and $\gamma = 1 + 1/n$, we find that $n = 3/2 = 1.5$. So for small values of x, the white dwarf is very closely approximated by an $n = 1.5$ polytrope.

Now, assume that the Fermi momentum is much greater than $m_\mathrm{e}c$, or that $p_\mathrm{f} \gg m_\mathrm{e}c$. In other words, the electrons are hyper-relativistic. This means that $x \gg 1$ because $x =$

$p_{\rm f}/(m_{\rm e}c)$. Because x is large,

$$f(x) \approx 2x^4$$

because $2x^4$ is the dominant term. Therefore

$$P_{\rm e} = \frac{\pi m_{\rm e}^4 c^5}{3h^3} 2x^4 = \frac{2\pi m_{\rm e}^4 c^5}{3h^3} \left(\frac{p_{\rm f}}{m_{\rm e}c}\right)^4 = \frac{2\pi c}{3h^3} p_{\rm f}^4.$$

Now by using Equation 2.16, the pressure due to degenerate electrons at large values of x, or hyper-relativistic velocities, is

$$P_{\rm e} = \frac{2\pi c}{3h^3} \left(\frac{3h^3}{8\pi} \cdot \frac{\rho}{\mu_{\rm e} m_H}\right)^{4/3} = \frac{(3\pi^2)^{1/3}}{8\pi} hc \left(\frac{\rho}{\mu_{\rm e} m_H}\right)^{4/3}. \tag{2.22}$$

Therefore $P_{\rm e} \sim \rho^{4/3}$. If we let $\gamma = 4/3$ and $\gamma = 1 + 1/n$, we find that $n = 3$. So for large values of x, the white dwarf is very closely approximated by an $n = 3$ polytrope.

Now that we have determined pressure due to electron degeneracy, we can apply it to find the specific internal energy. Using Equation 2.9 and Equation 2.20, we find that the specific internal energy is

$$u = \frac{c^2 m_{\rm e}(6x^5 + x^3(9 - 8(1+x^2)^{1/2}) + 3x - 3(1+x^2)^{1/2} \sinh^{-1} x)}{8 m_{\rm H} x^3 (1+x^2)^{1/2}}. \tag{2.23}$$

Equation 2.23 can be expressed in a much more convenient way. Notice that Equation 2.23 has some similarities to Equation 2.16 and Equation 2.17. By solving for ρ in terms of $p_{\rm f}$, we find that Equation 2.23 becomes

$$u = \frac{c^2 m_{\rm e}(x^2 - (1+x^2)^{1/2} + 1)}{m_{\rm H} \mu_{\rm e} (1+x^2)^{1/2}} - \frac{p_{\rm f}}{\rho}. \tag{2.24}$$

2.3.2 Chandrasekhar Mass Limit

The Chandresekhar mass limit is the maximum possible mass of a white dwarf. The largest mass of a white dwarf also corresponds to hyper-relativistic electrons inside the white dwarf. Therefore, by finding the largest possible mass of our $n = 3$ polytrope, we will find determine the largest mass possible for a white dwarf.

We begin with the integral definition of mass:

$$M = \int_0^R 4\pi r^2 \rho \, dr.$$

Now we use Equation 2.13 and Equation 2.14 to rewrite the integral in terms of ξ and θ^n. So the integral becomes

$$M = 4\pi \lambda_n^3 \rho_c \int_0^{\xi_1} \xi^2 \theta^n \, d\xi.$$

By using the Lane-Emden equation, Equation 2.15, we find that

$$M = -4\pi \lambda_n^3 \rho_c \int_0^{\xi_1} \frac{d}{d\xi}\left(\xi^2 \frac{d\theta_n}{d\xi}\right) d\xi.$$

We are able to simplify the integral because

$$\int_0^{\xi_1} \frac{d}{d\xi}\left(\xi^2 \frac{d\theta_n}{d\xi}\right) d\xi = -\xi_1^2 |\theta_n'(\xi_1)|,$$

where $\theta' \equiv \frac{d\theta_n}{d\xi}$. Also, by using Equation 2.14 to substitute λ_n, we know that

$$M = 4\pi \left[\frac{(n+1)K}{4\pi G}\right]^{3/2} \rho_c^{(3-n)/2n} \, \xi_1^2 |\theta_n'(\xi_1)|. \tag{2.25}$$

Note that K comes from Equation 2.10. Therefore for $n = 3$ and using our pressure due to hyper-relativistic degenerate electrons, Equation 2.22,

$$K = \frac{(3\pi^2)^{1/3}}{8\pi} hc \left(\frac{1}{\mu_e m_H}\right)^{4/3}.$$

Thus letting $n = 3$ and making the above substitution for K,

$$M_{\text{Ch}} = \frac{\sqrt{3\pi}}{2}\left(\frac{hc}{2\pi G}\right)^{3/2}\frac{1}{(\mu_{\text{e}}m_H)^2}\,\xi_1^2|\theta_n'(\xi_1)|$$

where M_{Ch} is the Chandrasekhar mass limit. Numerical integration of the Lane-Emden equation, Equation 2.15, gives $\xi_1^2|\theta_n'(\xi_1)| \approx 2.01824$ for $n = 3$. Let $\xi_1^2|\theta_3'(\xi_1)| = \omega_3^0 \approx 2.01824$. Then

$$M_{\text{Ch}} = \frac{\omega_3^0\sqrt{3\pi}}{2}\left(\frac{hc}{2\pi G}\right)^{3/2}\frac{1}{(\mu_{\text{e}}m_H)^2} \approx 1.44\,\text{M}_\odot \text{ [12]}. \tag{2.26}$$

The Chandrasekhar mass limit plays an important role in type Ia supernovae. When a white dwarf is in a binary system with another star, it is possible for the white dwarf to accrete matter from its companion star. If the white dwarf gains enough mass to reach the Chandrasekhar mass, the white dwarf will collapse and create a type Ia supernova.

2.4 Black Holes

Isaac Newton believed that light was a particle. In 1783 an English clergyman and astronomer, John Michell (1724-1793), believed that a star with the gravity of five hundred times that of the sun, but with the same average density of the Sun would have a force of gravity large enough that not even light could escape.

As the name suggests, black holes are black. The gravitational force is so strong that not even light can escape. The boundary at which light cannot escape is called the event horizon. Black holes are formed from the death of stars greater than approximately $15\,\text{M}_\odot$. The core of the dead stars are so dense that they collapse in on themselves similar to a white dwarf. The difference is that electron degeneracy pressure cannot support it. Not even neutron degeneracy pressure, the primary support of neutron stars, is strong enough. It is believed that the mass of a black hole is concentrated into an infinitely dense point at the center called a singularity.

Black holes are usually found in two different places. Stellar mass black holes, around 5 to 80 solar masses, are typically found within dense star forming regions [18]. This is because the more massive stars in the cluster become black holes quickly and are typically detected by the X-rays emitted by their accretion disks [19]. Supermassive black holes are typically found at the centers of galaxies. They are upwards of billions of solar masses. The most famous supermassive black hole is the one at the center of our Milky Way galaxy, Sagittarius A*, with a mass of around 4 million solar masses.

2.4.1 Schwarzschild Radius

The Schwarzschild radius of an object is the radius of sphere with the same mass that would collapse into a black hole. It is also the radius of the event horizon of a non-rotating, uncharged black hole. The calculation for the Schwarzschild radius is surprisingly simple. We want to know the radius at which light can just barely escape from a black hole. So we want our escape velocity to be the speed of light. So by setting the speed of light as our escape velocity in Equation 2.7 and solving for the radius, we find that

$$r_{\mathrm{s}} = \frac{2GM}{c^2}. \tag{2.27}$$

Although the derivation just sketched used Newtonian mechanics, the result turns out to be correct even in full general relativity [11].

2.5 Other Physics

2.5.1 Tidal Forces

Because stars are not point masses, gravity from another body does not have the same magnitude at every point in the star. The force differential is known as a tidal force. It is very pronounced in encounters with black holes due to the small radius of the event horizon.

It can be shown that along the line connecting the centers of a star and a black hole, the force differential is

$$\Delta\mathbf{F} = -\frac{2GM_{bh}mR_*}{r^3}\hat{\mathbf{r}}, \tag{2.28}$$

where m is the mass of a test particle at the surface of the star, M_{bh} is the mass of the black hole, R_* is the radius of the star, and r is the distance between the center of the star and the black hole.

It is possible for the force differential to be so great that chunks get ripped off of the star. This occurs when the object deforms so much that it overflows its Roche limit. The Roche limit for a star and black hole system occurs when the tidal force from the black hole has a greater force on a part of the star than the star does on that part. Therefore, if we assume that there are no intermolecular forces, we can set up the following inequality to represent when a test mass is no longer bound to the star by using Equation 2.4 and Equation 2.28:

$$\frac{GM_*m}{R_*^2} < \frac{2GM_{bh}mR_*}{r^3}.$$

By solving for r and simplifying, we find that the Roche limit is at a radius of

$$r_{\text{lim}} = 2^{1/3}\left(\frac{M_{bh}}{M_*}\right)^{1/3}R_*.$$

When doing a more thorough analysis, such as accounting for the deformation of the object, the constant of $2^{1/3} \approx 1.3$ was found to have a value of approximately 2.456. Making this correction, a star will have a partial tidal disruption if

$$r < 2.456\left(\frac{M_{bh}}{M_*}\right)^{1/3}R_*. \tag{2.29}$$

It has also been shown that if star comes to within about half of its Roche Limit, it experiences a complete tidal disruption where the star is completely ripped about by tidal forces.

Chapter 3

Methodology

3.1 Smoothed Particle Hydrodynamics

Smoothed Particle Hydrodynamics (SPH) is a method used to simulate the behavior of fluids. Blobs of fluid, or particles, are moved around by forces in small steps of time. The force applied to the fluid blob gives the blob an acceleration. The acceleration changes the velocity. The velocity changes the position. The internal energy of the fluid is also evolved [20].

Ideally, a particle will experience the interactions of all other particles. When there are thousands of particles, the computational power required would be enormous. So instead of interacting with all particles, they only experience non-gravitational interactions from particles around them. Any pressure forces are due to particles in the immediate vicinity of the particle in question. The particles that interact are called nearest neighbors. The sphere of self-influence contains about the same number of nearest neighbors for each particle. The radius of the sphere of self-influence is double the parameter called the smoothing length, h.

3.1.1 The Fundamentals

The engine of SPH is the interpolation that allows for any function to be expressed as a set of particles. We define the integral interpolant of a function $A(\mathbf{r})$ as

$$A_{\mathrm{I}}(\mathbf{r}) = \int A(\mathbf{r}')W(\mathbf{r}-\mathbf{r}', h)\mathbf{dr}', \tag{3.1}$$

where we are integrating over all space and W is the interpolating kernel. The kernel W is a function that has the following properties:

1. $\int W(\mathbf{r}-\mathbf{r}', h)\mathbf{dr}' = 1$ and
2. $\lim_{h\to 0} W(\mathbf{r}-\mathbf{r}', h) = \delta(\mathbf{r}-\mathbf{r}')$

where δ is the normalized Dirac delta function [20].

Computationally, unless you already have an antiderivative, it is not possible to find an analytic solution to Equation 3.1. Therefore, we approximate the integral interpolant with the summation interpolant

$$A_S(\mathbf{r}_a) = \sum_b m_b \frac{A_b}{\rho_b} W(\mathbf{r}_a - \mathbf{r}_b, h_a) \tag{3.2}$$

where the summation index b is a particle label and the summation is over all particles. So particle b has mass m_b, density ρ_b, position $\mathbf{r}_b$ and the quantity A_b which is the value of A at $\mathbf{r}_b$ [20]. We can also construct a differentiable interpolant of a function from its values at the particles. We do this by using a differentiable kernel W. Interpolant derivatives are found by ordinary differentiation. So to find ∇A, we have

$$\nabla A(\mathbf{r}_a) = \sum_b m_b \frac{A_b}{\rho_b} \nabla W(\mathbf{r}_a - \mathbf{r}_b, h_a). \tag{3.3}$$

We now have our basic interpolants [20].

A common kernel to use for W is the cubic spline kernel seen in Figure 3.1. The cubic

spine kernel is defined as

$$W(\mathbf{r},h) = \frac{\sigma}{h^{\nu}} \begin{cases} 1 - \frac{3}{2}\left(\frac{r}{h}\right)^2 + \frac{3}{4}\left(\frac{r}{h}\right)^3 & \text{if } 0 \leq \frac{r}{h} \leq 1; \\ \frac{1}{4}\left(2 - \frac{r}{h}\right)^3 & \text{if } 1 \leq \frac{r}{h} \leq 2; \\ 0 & \text{otherwise} \end{cases} \tag{3.4}$$

where ν is the number of dimensions and σ is a normalization constant with values of $\frac{2}{3}$, $\frac{10}{7\pi}$, $\frac{1}{\pi}$ for one, two, and three dimensions respectively. A main advantage of using this kernel is that interactions are exactly 0 for $r > 2h$. Therefore, the only particles that non-gravitationally affect a test particle are those within a distance of $2h$ [20].

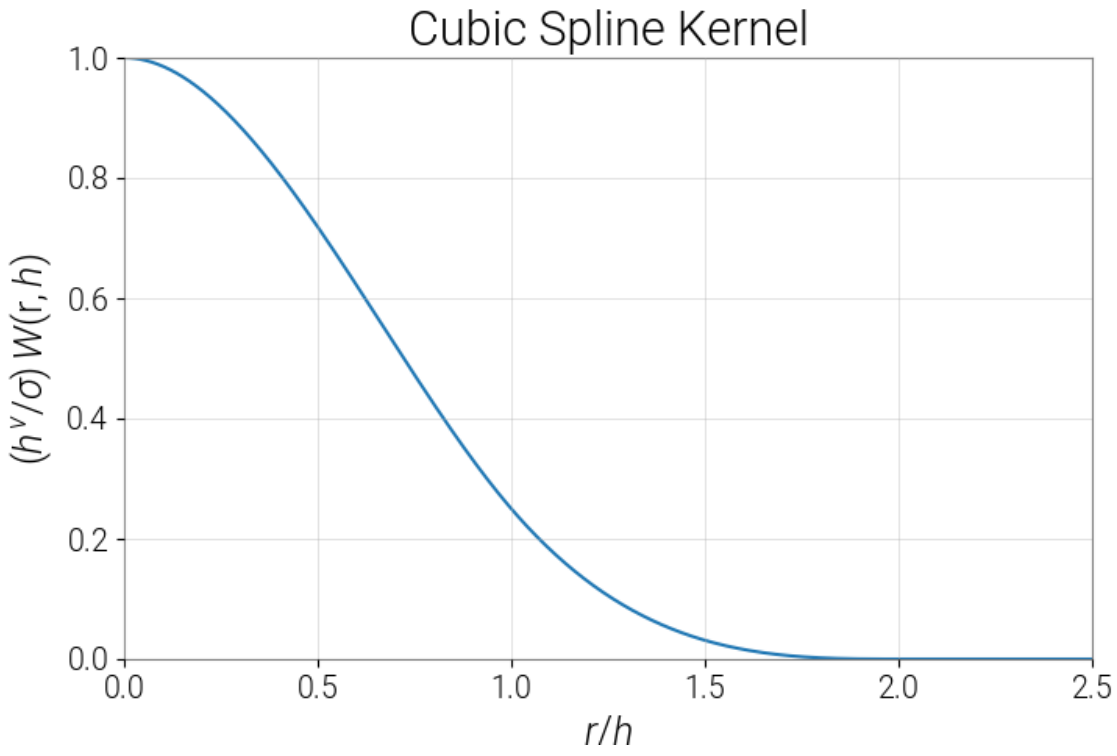

Figure 3.1: Graph showing the non-constant portion of the cubic spline function. Note that the Weighting funtion reaches exactly 0 at $r/h = 2$.

There are four main equations that govern the physical quantities of a particle. The quantities are density, acceleration, internal energy, and velocity. We estimate the density

by

$$\rho(\mathbf{r}_a) = \sum_b m_b W(\mathbf{r}_a - \mathbf{r}_b, h_a). \tag{3.5}$$

We define $\rho_a = \rho(\mathbf{r_a})$. From Euler's equation of hydrodynamics, we find the acceleration of particle a to be

$$\frac{d\mathbf{v}_a}{dt} = -\sum_b m_b \left(\frac{P_b}{\rho_b^2} + \frac{P_a}{\rho_a^2}\right) \nabla_a W_{ab} \tag{3.6}$$

where $\nabla_a W_{ab}$ is the gradient of $W(\mathbf{r} - \mathbf{r}', h)$ taken with respect to the coordinates of particle a. Equation 3.6 is known as the momentum equation of particle a. By multiplying each side by the mass of particle a, we have the change in momentum which is the force by Equation 2.2. Along with the fact that the summand on the right side of Equation 3.6 is antisymmetric, we conserve momentum and follow Newton's third law, Equation 2.3.[1] From the first law of thermodynamics, the rate of change in the internal energy of particle a is

$$\frac{du_a}{dt} = \frac{1}{2}\sum_b m_b \left(\frac{P_b}{\rho_b^2} + \frac{P_a}{\rho_a^2}\right) \mathbf{v}_{ab} \cdot \nabla_a W_{ab} \tag{3.7}$$

where $\mathbf{v}_{ab}$ is the velocity of particle a with respect to particle b. Particles are moved by

$$\frac{d\mathbf{r}_a}{dt} = \mathbf{v}_a. \tag{3.8}$$

So the particles are in a distribution where there is a pressure, which causes an acceleration, which causes the velocity to change which will change the position [20].

There is one more change that must be made to these equations. There should be an artificial viscosity associated with each particle to prevent particles from moving through each other when they should not be doing so. The most common artificial viscosity is a correction to the acceleration of a particle

$$\frac{d\mathbf{v}_a}{dt} = -\sum_b m_b \left(\frac{P_b}{\rho_b^2} + \frac{P_a}{\rho_a^2} + \Pi_{ab}\right) \nabla_a W_{ab} \tag{3.9}$$

[1] A function f is antisymmetric if $f(a, b) = -f(b, a)$.

where

$$\Pi_{ab} = \begin{cases} \dfrac{-\alpha \bar{c}_{ab} \mu_{ab} + \beta \mu_{ab}^2}{\bar{\rho}_{ab}} & \mathbf{v}_{ab} \cdot \mathbf{r}_{ab} < 0; \\ 0 & \mathbf{v}_{ab} \cdot \mathbf{r}_{ab} > 0 \end{cases}$$

and defining

$$\mu_{ab} = \frac{h \mathbf{v}_{ab} \cdot \mathbf{r}_{ab}}{\mathbf{r}_{ab}^2 + \eta^2}.$$

In Equation 3.9, α, β, and η are constants while $\bar{c}$ is the average sound speed and $\bar{\rho}$ is the average density [20].

3.1.2 Using *Starsmasher*

Starsmasher is a three-dimensional smoothed particle hydrodynamics (3dSPH) code that is used to simulate collisions between stars or other compact objects. It is currently maintained by Dr. James Lombardi, Jr and collaborators.[2] The equations used in *Starsmasher* are similar to those mentioned in Section 3.1.1 and are outlined in Gaburov et al. 2010 [21].

The first step of beginning a simulation is to relax each star. We have *Starsmasher* lay down particles in an organized manner that roughly follows the given equation of state as well as the desired density and specific internal energy profiles. From here, we run the simulation and let the star reach hydrostatic equilibrium via Equation 2.11. While a star is relaxing we check the energy of the relaxation to make sure that there are no unforeseen changes in the energy. An example of the energy graph for 30 code units of time, where one code unit of time is 0.018445 days, is seen in Figure 3.2. In the first few units of time, there is oscillation due to the movement of particles reaching equilibrium. Notice that the total energy of the relaxation has a slight increase in energy at late times. The incremental increase in energy is due to numerical integration and can be made smaller by using smaller timesteps. Overall, we look for a change of no more than 1%. In this particular run, we have very good energy conservation. Also, notice that there is very steep drop in the kinetic

[2]The most current version of *Starsmasher* can be found on GitHub (`https://github.com/jalombar/starsmasher`).

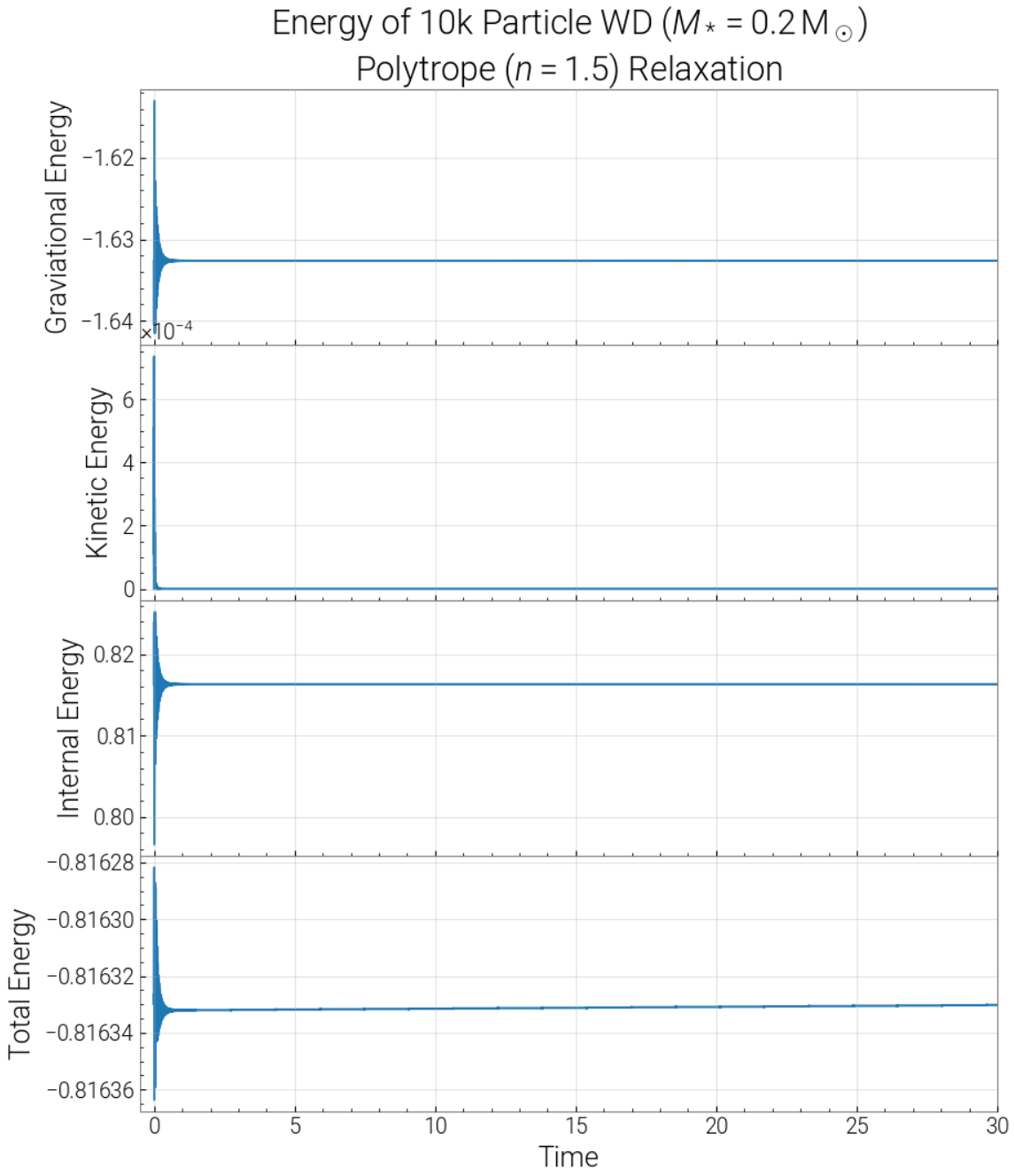

Figure 3.2: Graph of energies for the relaxation of a ten-thousand particle run of a $0.2\,M_\odot$ $n = 1.5$ polytrope. We consider this a successful relaxation. For a successful relaxation, we look at things such as energy conservation and continuity of the energy curves.

energy of our system at early times. This is because *Starsmasher* can add an extra drag force to relaxation runs. In the polytropic runs, the drag force exists for the first 0.25 code units of time. This is because there can be a large amount of movement at the beginning of a relaxation run, and we do not want particles to move too much between time steps. Once we know that we have a successful relaxation, we move onto the dynamical simulation.

Dynamical simulations in *Starsmasher* usually involve two bodies, although triples have been simulated using *Starsmasher* before. In this case, we only used a single input, either the polytropic representation of a white dwarf or a white dwarf using an electron degeneracy equation of state. We use an out-file produced by a relaxation run as the starting point for a dynamical run. We want to make sure that the star reaches equilibrium before bringing it over into the dynamical run. Therefore, we want to pick a later out-file. However, we do not want to pick the last out file because of the small energy increase that we get over time. So we should choose a middle value such as out-file 20 or 30. At this point in time, there are no noticeable oscillations and there has been a negligible increase in the total energy. By default, *Starsmasher* uses a black hole as the other body if it is not specified.

In *Starsmasher*, we approximate black holes with a single particle with the mass of the black hole. Whenever other particles are far away, more than twice the smoothing length of the black hole particle, the black hole particle acts like a point mass. The gravity is softened inside $2h$ for black hole particles in the same way as standard SPH particles. Also, there is no pressure due to black hole particles. In most cases, we do not need to worry about the event horizon because it would be well inside the radius of our particle.[3]

3.2 Initial Conditions

In all simulations, a black hole mass of $10\,\mathrm{M}_\odot$ was used. The smoothing length of the black hole is set to $0.0022\,\mathrm{R}_\odot$.

[3]See Section 2.4.1.

3.2.1 Polytropic Equation of State

The test polytropes that were made to represent white dwarfs are all of mass $0.2\,M_\odot$. This low of a mass is represented by $n = 1.5$ polytropes. So we set $\gamma = 1 + 1/n = 5/3$. We estimated the radius of the white dwarf to be $0.021\,R_\odot$. We have four WD-BH simulations: two ten-thousand particle runs and two one-hundred thousand particle runs. In each of those categories, we have an impact parameter of 0.1 $R_\odot$ for a partial tidal disruption and 0.06 $R_\odot$ for a complete tidal disruption.

3.2.2 Electron Degeneracy Equation of State

We use the central value of x from Section 2.3.1 as an input and let the code do the rest. From the central value of x, we are able to calculate the final mass as well as the radius of the star. In the only simulation using the electron degeneracy equation of state, we use a central x value of one. A central x value of one corresponds to a mass of 0.51 $M_\odot$ and a radius of 0.01394 $R_\odot$. If we had a white dwarf with the same radius used in our polytropic run, $0.021R_\odot$, we would have mass of 0.201 $M_\odot$ and a central x value of 0.4635. If we had a white dwarf with the same mass used in our polytropic run, 0.2 $M_\odot$, we would have a radius of 0.02106 $R_\odot$ and a central x value of 0.461.

3.2.3 Edge Particle Placement

When *Starsmasher* places particles down to form a star, we want to have particles placed so that they are as close to equilibrium as possible. Because each particle has a smoothing length, we do not want to place particles at the full radius of the star because this would create a star that is slightly too large. Therefore, we place particles such that they are a certain number of smoothing lengths from the radius. In many other versions of *Starsmasher*, we stop placing particles at three times the smoothing length from the calculated radius. This seemed a little drastic so I lowered that value to a single smoothing length from the

calculated radius.

3.2.4 Relaxation Drag Force

When performing a relaxation in *Starsmasher*, it is common to add an artificial drag force at the start of the run. The drag is used to temporarily decrease the amount of movement that articles experience that they reach equilibrium. In other words, it would decrease the relaxation time and allow for more reliable relaxations at the cost of energy conservation. Since *Starsmasher* was first written, there have been many improvements to the code that allow for more aggressive relaxations and stability is not an issue. Therefore in my relaxation runs with electron degeneracy pressure, I do not include any time with the artificial drag force.

3.2.5 Number of Neighbors

The number of neighbors is the amount of surrounding particles used to calculate quantities such as pressure. We want to try and keep the number of neighbors as consistent as possible throughout the runs. A change in the number of neighbors, particularly between the relaxation and dynamical run, may result in movement within the star. We do not want to have a rigid number of neighbors though, as that would result in smoothing lengths getting very small when particles condense or smoothing lengths becoming very large in low density environments. In the code, the variable that controls the ideal number of neighbors is `NNOPT` which is set to 39 for all of the runs which results in the average number of neighbors of 54.

Chapter 4

Results and Analysis

4.1 Polytropes

I ran multiple simulations involving black holes using an $n = 1.5$ polytrope to make sure that the *StarSmasher* was running properly. Screenshots from a completed run is seen below in Figure 4.1. There was no artificial drag force used in the relaxtion of the polytropes and we used the smaller `redge` value to place particles closer to the calculated edge of the star. This project was focusing more on the electron degeneracy set of runs as these had not been implemented in *StarSmasher* before.

4.2 Electron Degeneracy

4.2.1 Internal Energy

Unlike other equations of state, zero-temperature electron degeneracy pressure is not dependent on the internal energy. Therefore, we can do whatever we want with the internal energy of the particles but that is not good practice. If we wanted to have a hybrid equation of states, such as including radiation pressure along with electron degeneracy, we would need to have an accurate internal energy from electron degeneracy. In our first attempt to do this,

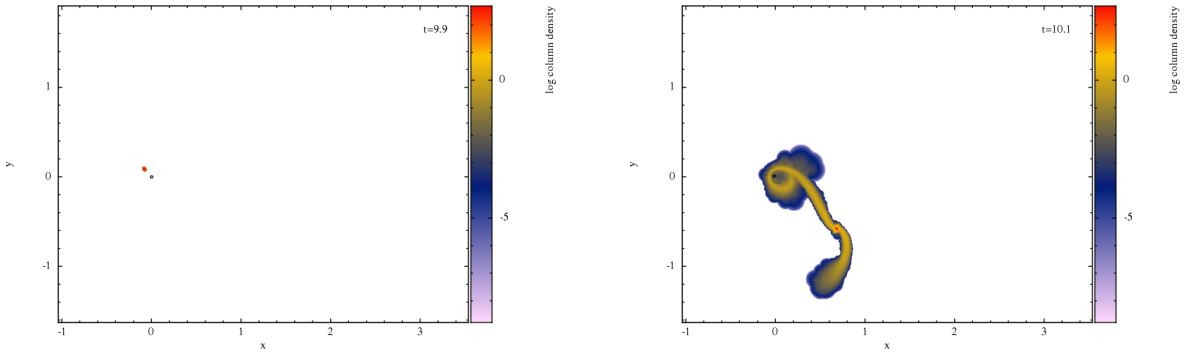

(a) $t = 9.9$ (b) $t = 10.1$

Figure 4.1: Shown here is the column densities during various parts of the collision between a ten-thousand particle 0.2 $M_\odot$ polytrope and a 10 $M_\odot$ black hole. The black hole is shown as a black circle. The periastron separation is 0.1 $R_\odot$ which is approximately the radius of the white dwarfs. The x-axis and y-axis are in solar radii. Time is in code units.

we were getting specific internal energies that became negative because the estimated value for the initial specific were presumably too small. One thing that we noticed is that the numerical evaluation for the internal energy, Equation 2.23, of a particle would oscillate very heavily at low values of x due to the $\sinh^{-1} x$ term. Thus, we used a Taylor expansion to approximate the value of the internal energies at the low value of x. The approximation can be seen in lines 88-90 of Appendix A.1. The implementation of the internal energy should be a good stepping stone for further integration of electron degeneracy in smoothed particle hydrodynamics.

4.2.2 Collisions with White Dwarfs

As a proof of concept, we decided to do a few simulations between two electron degeneracy white dwarfs. We did this to ensure that any complications that we see in the black hole runs would be due to the black hole and not the code associated with electron degeneracy. Also, we cannot do a collision between a polytrope and a white dwarf as they have different equations of state. We do not have one equation that would allow for both the polytrope and white dwarf to exist at the same time. So for both of the white dwarfs, we used the

central x of 1 white dwarfs and collided them. As stated in Section 3.2.2, each white dwarf was 0.510066 $M_\odot$ so even if all of the mass was bounded after the collision, we would have a final mass after the collision of well within the Chandrasekhar Mass Limit. In the end, we had successful runs using both the limited-h and the non-limited-h code. A plot of the column densities can be seen in Figure 4.2 while the energies for the simulation can be seen in Figure 4.3.

4.2.3 Collisions with Black Holes

Due to the limitations of using only electron degeneracy pressure to calculate pressure, if we do not want to simulate collisions between two white dwarfs, we must use a black hole as our second body. The runs involving black holes did not go as smoothly as those involving two white dwarfs. The issue that once the white dwarf undergoes a partial tidal disruption, particles collapse onto the black hole and the time steps get extremely small. This behavior can occur when the smoothing lengths are allowed to approach zero. Small smoothing lengths allow the particles to get close together so addressing the smoothing length could take care of the small time steps.

Sarah Seitanakiss's version of the code, nicknamed "limited-h", sets a maximum and minimum value to the smoothing lengths of each particle. Using this version of the code did not make any large scale improvements. After the tidal disruption, particles still fell onto the black hole and time steps became small. However, instead of the time steps approaching zero, once they got to about 1×10^{-7} time units per time step, the code stopped. We do not have a solution to the time step issue at the current time as bug fixing a large program such as *StarSmasher* takes a large amount of time. However we were able to narrow the issue down to the last 1/12 of particle numbers as we split the calculations up into 12 groups.

StarSmasher is a parallelized code. So *StarSmasher* does independent calculations on different sets of particles using multiple pieces of hardware. Once the calculations are complete, they must all be compiled back onto a single piece of hardware to create the log files.

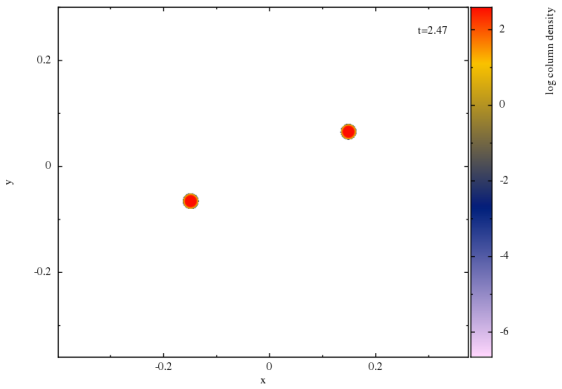

(a) $t = 2.47$

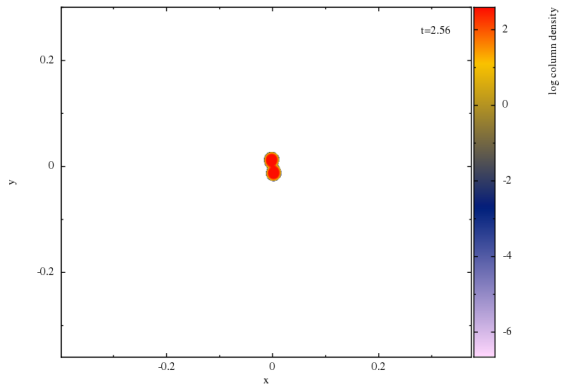

(b) $t = 2.56$

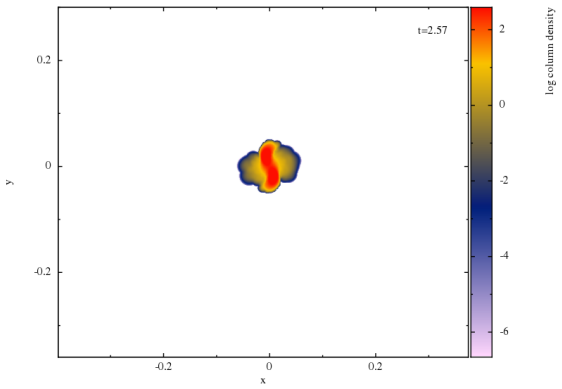

(c) $t = 2.57$

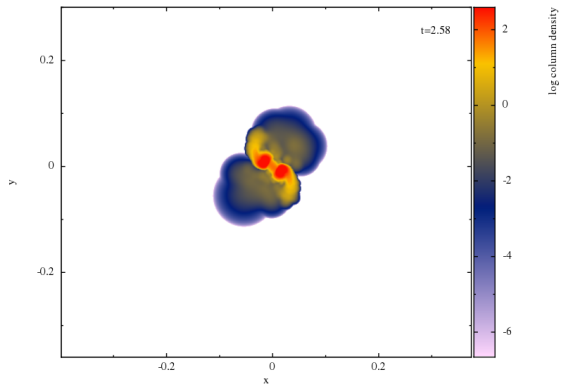

(d) $t = 2.58$

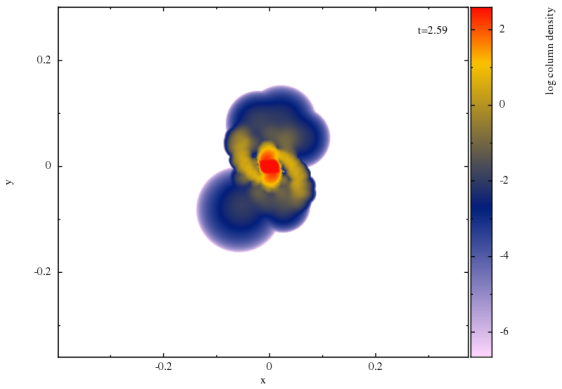

(e) $t = 2.59$

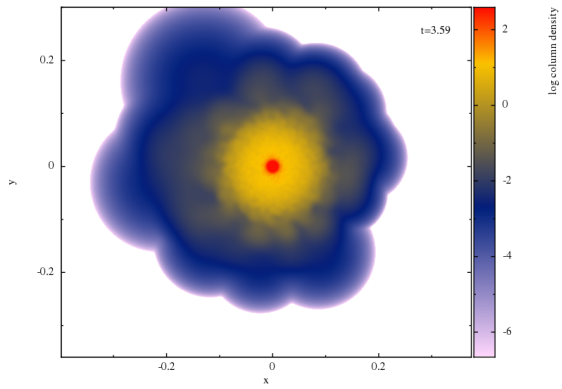

(f) $t = 3.59$

Figure 4.2: Shown here is the column densities during various parts of the collision between two ten-thousand particle 0.51066 $M_\odot$ zero-temperature electron degeneracy white dwarfs. The periastron separation is 0.014 $R_\odot$ which is approximately the radius of the white dwarfs. The x-axis and y-axis are in solar radii. Time is in code units.

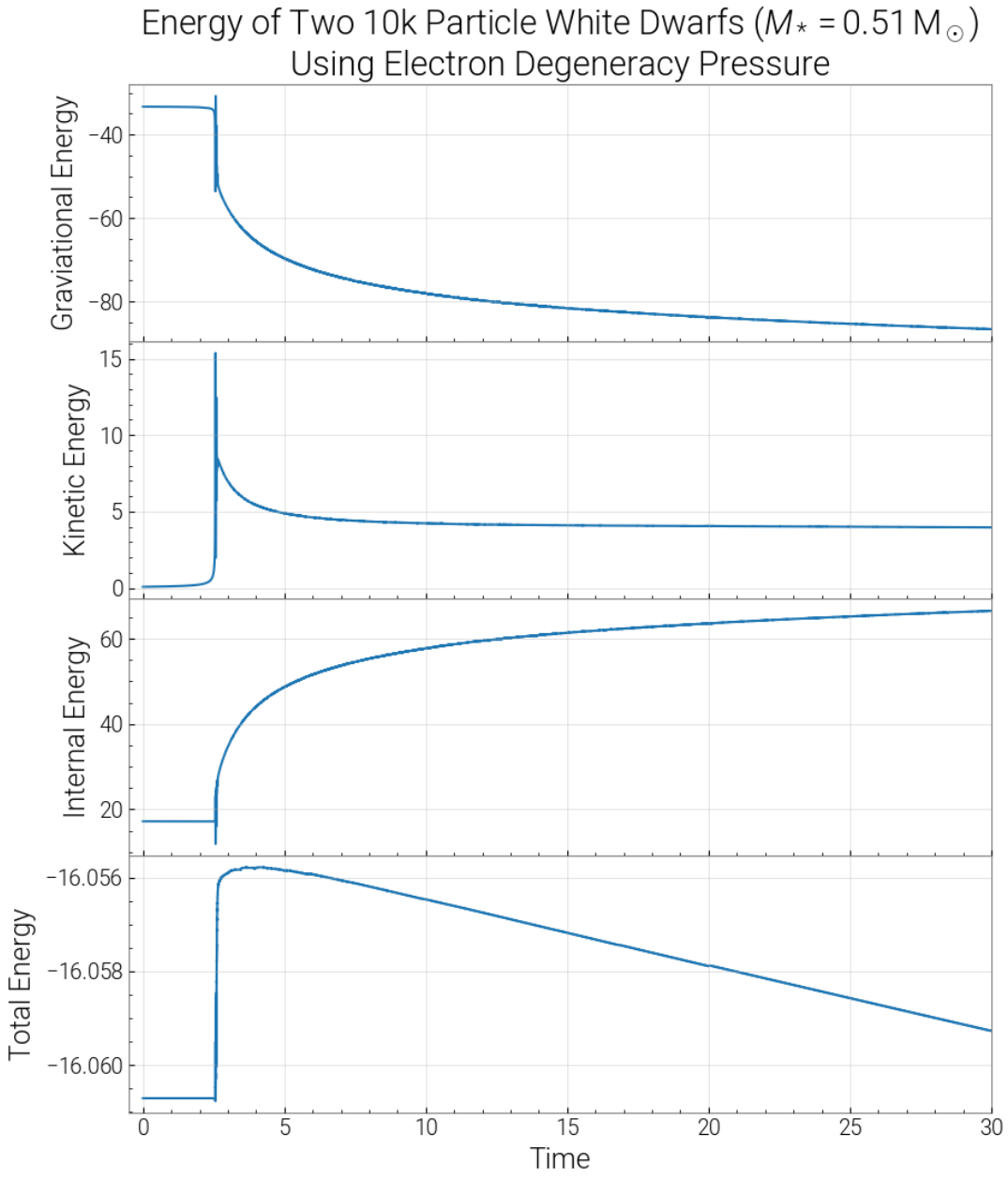

Figure 4.3: Graph of energy for the collision of two ten-thousand particle white dwarfs using zero-temperature electron degeneracy. They are each 0.51066 $M_\odot$. Time is is code units.

In our case, we had twelve processes all running simultaneously. The calculations involving the final set of particles did not complete fully. We noticed that it was not even getting to the portion of the code that involved compiling the results from the rest of the processes. Our current understanding of the situation is that the code is waiting for the last process to report its values but it never happens. [1] Therefore the code stalls.

Regardless of the exact cause of the halted code, we need to find a way to avoid particles getting that close to begin with. This could be achieved by implementing a more complicated equation of state equation of state. Zero-temperature electron degeneracy pressure dominates pressure calculations only when particles are very close to each other. When particles are torn away from the white dwarf, they are no longer in a very dense environmet. I believe that the particles that are stripped from the white dwarf and fall down towards the black hole are not packed closely enough for the electron degeneracy pressure to contribute much at all. Therefore, the particles are in free fall and barely interact with each other and the particles just keep getting closer and closer together. If there are other sources of pressure, it may be enough to prevent particles from reaching the black hole in such a timely fashion.

[1] More details can be found in Appendix A.4: Debugging Progress.

Chapter 5

Conclusion

Overall, this project had the objective of simulating middle-mass white dwarfs using electron degeneracy pressure. Before this work, the three-dimensional smoothed particle hydrodynamics code *StarSmasher* could only approximate low mass and high mass white dwarfs using $n = 1.5$ and $n = 3$ polytropes respectively. *StarSmasher* is now able to use the equations outlined in Section 2.3.1 to calculate the pressure due to degenerate electrons. This allows for white dwarfs that are not proportional to $\rho^{5/3}$ or $\rho^{4/3}$ to be represented in *StarSmasher*.

We began the implementation by representing low mass white dwarfs with an $n = 1.5$ polytrope. We then researched zero-temperature electron degeneracy pressure to implement it inside *StarSmasher*. As a proof of concept, we collided two of these zero-temperature electron degeneracy white dwarfs without any complication. Attempting to collide one of these white dwarfs with a black hole represented by a point mass did not go as smoothly. We have an issue where particles fall down onto the black hole particle so much that the time steps become extremely small. Even if they do not become seemingly infinitely small, the code would crash even when using a version of the code that would limit the smoothing length allowed by particles. In the end, we were successful in using zero-temperature electron degeneracy pressure to simulate a white dwarf in *StarSmasher*.

5.1 Future Works

Other groups can expand upon this research by looking at white dwarfs colliding with other objects. We know that white dwarfs get close enough to other stars to accrete matter which may result in a type Ia supernova [22]. Therefore it is not unreasonable to expect collisions to occur with either main sequence stars or other white dwarfs. To do simulations involving a white dwarf and a main sequence star, we must have a more complex pressure equation as we would need electron degeneracy to be an addition to the pressures that exist within other stars such as radiation pressure. Before someone can attempt to create this more complex pressure equation, they would need to make sure that the specific internal energy of the particles is initialized correctly. We did not have to spend much time dealing with internal energy because zero-temperature electron degeneracy pressure is independent of the internal energy of the particle. Other forms of pressure may be dependent on internal energy so it must be assigned more carefully.

The study can also be looked at in the context of star clusters. Many collisions are believed to occur in star clusters. It is possible that a large majority of white dwarf collisions would occur in the high stellar density environment of clusters. Because we have observed the collisions of binary neutron stars, it is not far-fetched to assume that there are binary white dwarf systems considering that we would expect there to be a larger population of white dwarfs throughout the cosmos.

Appendix A

Code

A.1 pressure.f

The portion of `pressure.f` that I added for electron degeneracy pressure was lines 74-95. Note that when implementing Equation 2.16, we used the fact that one gram of hydrogen is equal to Avagradro's number of atoms per gram. When x gets low, we use an approximation because Equation 2.20 becuase at low values of x, the values become too small for the code the handle accurately.

```
1       subroutine pressure
2       include 'starsmasher.h'
3       real*8 pgas,prad
4       real*8 rhocgs,ucgs,beta1,temperature,gam1,useeostable
5       real*8 fx,pF,xF
6       integer i
7       real*8 mue
```

```
74      else if(neos.eq.3) then
75         do i=n_lower,n_upper
76            if(u(i).ne.0.d0) then
77               rhocgs=rho(i)*munit/runit**3.d0
78
```

```
79        !For now, just set mue=2.  This will need generalized later.
80                mue=2d0
81
82                xF=(3*Na/(8*mue*pi)*rhocgs)**(1d0/3)*planck/(crad*melec)
83                if(xF.gt.7.806834220522274d-2) then
84                   por2(i)=(crad**5*melec**4*pi*(xF*Sqrt(1 + xF**2)
85     $                  *(-3 + 2*xF**2)
86     $                  + 3*log(xF+Sqrt(1+xF**2)))/(3*planck**3))/punit/rho
   (i)**2
87                else
88                   por2(i)=(8*crad**5*melec**4*pi*xF**5/(15*planck**3)
89     $                  *(1+xF**2*(-5d0/14+xF**2*
90     $                  (5d0/24-25d0/176*xF**2))))/punit/rho(i)**2
91                endif
92             else
93                por2(i)=0.d0
94             endif
95          enddo
96       endif
97
98       return
99       end
```

A.2 initialize_parent.f

```
850       else if(neos.eq.3) then
851          xF=(3*Na/(8*muearray(i)*pi)*rhoarray(i))**(1d0/3)*planck/(crad*
   melec)
852          uarray(i)=-pres(i)/rhoarray(i)
853     $         + Na*crad**2*melec*(-1+Sqrt(1+xF**2))/(gram*muearray(i))
```

A.3 White Dwarf Profile Integration

This is the main file that creates an input for *StarSmasher*. It gives the initial densities, masses, and starting positions of the particles. We must run this with the desired central x value. The routines that are called within this file are double precision versions of those from *Numerical Recipes in Fortran77* [23].

```
      PROGRAM xodeint
      implicit none
C     driver for routine odeint
      INTEGER KMAXX,NMAX,NVAR
      PARAMETER (KMAXX=10000,NMAX=50,NVAR=3)
      INTEGER i,kmax,kount,nbad,nok,nrhs
      real*8 dxsav,eps,h1,hmin,x1,x2,x,y,ystart(NVAR)
      COMMON /path/ kmax,kount,dxsav,x(KMAXX),y(NMAX,KMAXX)
      COMMON nrhs
      EXTERNAL derivs,rkqs
      real*8 xc,atilde,density,runit,munit,pressure,u
      real*8 avogadro,pi,mue,gram,sec,cm,me,planck,gravconst,crad
      parameter(avogadro=6.022140857d23,
     $     pi=3.14159265358979323846264338328d0,
     $     mue=2,
     $     gram=1,
     $     cm=1,
     $     sec=1,
     $     me=9.10938356d-28*gram,
     $     planck=6.6260755d-27*gram*cm**2/sec,
     $     gravconst = 6.67390d-08*cm**3/gram/sec**2,
     $     crad=2.997924580d+10*cm/sec,
     $     runit=6.9599d10*cm,
     $     munit=1.9891d33*gram)
      real*8 dpressuredx,g

```

```
27       nrhs=0
28       xc=1.d0
29       atilde=3*avogadro/(4*pi*mue*gram*me)*
30      $     sqrt(planck**3/(gravconst*crad*xc))/(1+xc**2)**0.25d0
31       print *,'Characteristic length in solar radii=',atilde/runit
32
33       eps=1.0d-12
34       h1=eps**0.5d0*atilde
35       x1=h1
36       x2=3*atilde
37       print *,'integrating from',x1/runit,'to',x2/runit
38
39       ystart(1)=xc*(1-(x1/atilde)**2)
40       ystart(2)=-2*xc*x1/atilde**2
41       density = 8*crad**3*gram*me**3*mue*pi*ystart(1)**3/
42      $     (3d0*avogadro*planck**3)
43       ystart(3)=4d0/3*pi*x1**3*density
44       hmin=0.0d0
45       kmax=10000
46       dxsav=(x2-x1)/10000.0d0
47       call odeint(ystart,NVAR,x1,x2,eps,h1,hmin,nok,nbad,derivs,rkqs)
48       write(*,'(/1x,a,t30,i5)') 'Successful steps:',nok
49       write(*,'(1x,a,t30,i5)') 'Bad steps:',nbad
50       write(*,'(1x,a,t30,i5)') 'Function evaluations:',nrhs
51       write(*,'(1x,a,t30,i5)') 'Stored intermediate values:',kount
52       write(*,'(/1x,t9,a,t20,a,t33,a,t46,a,t59,a,t72,a,t85,a,t98,a)')
53      $     'r/rsun','x','dx/dr','density','-dP/dr/g','m/msun',
54      $     'pressure','u'
55       do i=1,kount
56          density = 8*crad**3*gram*me**3*mue*pi*y(1,i)**3/
57      $        (3d0*avogadro*planck**3)
58          if(y(1,i).gt.7.806834220522274d-2) then
59             pressure=crad**5*me**4*pi*(y(1,i)*Sqrt(1 + y(1,i)**2)
```

```
60      $            *(-3 + 2*y(1,i)**2)
61      $            + 3*log(y(1,i)+Sqrt(1+y(1,i)**2)))/(3*planck**3)
62           else
63 c             print *,'Using approximation'
64              pressure=8*crad**5*me**4*pi*y(1,i)**5/(15*planck**3)
65      $         *(1+y(1,i)**2*(-5d0/14+y(1,i)**2*
66      $            (5d0/24-25d0/176*y(1,i)**2)))
67           endif
68           u = -pressure/density
69      $         + avogadro*crad**2*me*(-1+Sqrt(1+y(1,i)**2))/(gram*mue)
70
71           dpressuredx=8*crad**5*me**4*pi*y(1,i)**4/(3*planck**3*
72      $         Sqrt(1 + y(1,i)**2))
73           g=gravconst*y(3,i)/x(i)**2
74
75           write(*,'(1x,g10.4,2x,9g14.6)') x(i)/runit,y(1,i),y(2,i),
76      $         density,-dpressuredx*y(2,i)/g,y(3,i)/munit,pressure,u
77           write(123,*) y(3,i),x(i),pressure,density,0,0,1,0,0,0,0,0,0
78        enddo
79
80        print *,'The Chandrasekhar mass limit is', 2.018236d0*sqrt(3*pi)
81      $     /2*(planck/(2*pi)*crad/gravconst)**1.5d0/
82      $     (mue*gram/avogadro)**2/munit,'msun'
83
84
85        END
86
87        SUBROUTINE derivs(x,y,dydx)
88        implicit none
89        INTEGER nrhs
90        real*8 x,y(*),dydx(*)
91        COMMON nrhs
92        real*8 density
```

```
93       real*8 avogadro,pi,mue,gram,sec,cm,me,planck,gravconst,crad
94       parameter(avogadro=6.022140857d23,
95      $     pi=3.14159265358979323846264338327950288419716939937510d0,
96      $     mue=2,
97      $     gram=1,
98      $     cm=1,
99      $     sec=1,
100     $     me=9.10938356d-28*gram,
101     $     planck=6.6260755d-27*gram*cm**2/sec,
102     $     gravconst = 6.67390d-08*cm**3/gram/sec**2,
103     $     crad=2.997924580d+10*cm/sec)
104      nrhs=nrhs+1
105c     x = r (the radius)
106c     y(1) = x (the electron degeneracy parameter, not the radius)
107c     y(2) = dx/dr
108c     y(3) = enclosed mass
109
110      dydx(1)=y(2)
111c       dydx(2)=-32*crad*gram**2*gravconst*me**2*mue**2*pi**2*y(1)**2*
112c     $     Sqrt(1 + y(1)**2)/(3*avogadro**2*planck**3)
113c     $     - 2*y(2)/x
114
115      dydx(2)=-y(2)*( 2*y(1)+x*y(2) ) /(x*y(1)*(1 + y(1)**2)) +
116     $     y(1)**2*(
117     $     -32*crad*gram**2*gravconst*me**2*mue**2*pi**2*Sqrt(1+y(1)**2)
118     $     /(3*avogadro**2*planck**3)
119     $     - 2*y(2)/(x*(1 + y(1)**2)))
120
121c      if(dydx(2).ne.dydx(2)) then
122c         print *, x,y(1),y(2)
123c         sToP
124c      endif
125
```

```
126
127       density = 8*crad**3*gram*me**3*mue*pi*y(1)**3/
128      $      (3d0*avogadro*planck**3)
129       dydx(3)=4*pi*x**2*density
130
131       return
132       END
```

A.4 Debugging Progress

When completing my comp, I was in the middle of debugging the limited-h version of the code. I was specifically looking at `advance.f90` which handles the calculations for each time step. I found that in the subroutine `rho_and_h`, the last set of processes would not reach the `do` loop on line 588. On Gonzales, we are able to run 12 sets of particles in parallel and the first 11 made it to this point but the final one did not. There is a reason that this occurred but I did not have to time to track down this particular issue. I placed several debug statements which you may find useful which can be found in the following path `/data2/lachatm/comp/wd_edp/dyn_tests/final_runs/comp_dyn_sarah_cnum3`.

Appendix B

Constants

Astronomical Constants [11]			
Solar Mass	$1\,\mathrm{M}_\odot$	$=$	$1.9891 \times 10^{30}\,\mathrm{kg}$
		$=$	$1.9891 \times 10^{33}\,\mathrm{g}$
Solar Radius	$1\,\mathrm{R}_\odot$	$=$	$6.955\,08 \times 10^{8}\,\mathrm{m}$
		$=$	$6.955\,08 \times 10^{10}\,\mathrm{cm}$

Physical Constants [11]			
Universal Gravitational Constant	G	$=$	$6.673 \times 10^{-11}\,\mathrm{N\,m^2\,kg^{-2}}$
		$=$	$6.673 \times 10^{-8}\,\mathrm{cm^3\,g^{-1}\,s^{-1}}$
Speed of Light	c	$=$	$2.997\,924\,58 \times 10^{8}\,\mathrm{m\,s^{-1}}$
		$=$	$2.997\,924\,58 \times 10^{10}\,\mathrm{cm\,s^{-1}}$
Planck Constant	h	$=$	$6.626\,068\,96 \times 10^{-34}\,\mathrm{J\,s}$
		$=$	$6.626\,068\,96 \times 10^{-27}\,\mathrm{g\,cm\,s^{-2}}$
Hydrogen Mass	m_H	$=$	$1.673\,532\,499 \times 10^{-27}\,\mathrm{kg}$
		$=$	$1.673\,532\,499 \times 10^{-24}\,\mathrm{g}$

Bibliography

1. Abbott, B. P. *et al.* Astrophysical Implications of the Binary Black-hole Merger GW150914. **818,** L22. arXiv: 1602.03846 [astro-ph.HE] (Feb. 2016).
2. Abbott, B. P. *et al.* Observation of Gravitational Waves from a Binary Black Hole Merger. **116,** 061102. arXiv: 1602.03837 [gr-qc] (Feb. 2016).
3. Abbott, B. P. *et al.* Tests of General Relativity with GW150914. **116,** 221101. arXiv: 1602.03841 [gr-qc] (June 2016).
4. Abbott, B. P. *et al.* Properties of the Binary Black Hole Merger GW150914. **116,** 241102. arXiv: 1602.03840 [gr-qc] (June 2016).
5. Abbott, B. P. *et al.* GW151226: Observation of Gravitational Waves from a 22-Solar-Mass Binary Black Hole Coalescence. **116,** 241103. arXiv: 1606.04855 [gr-qc] (June 2016).
6. Abbott, B. P. *et al.* Binary Black Hole Mergers in the First Advanced LIGO Observing Run. *Physical Review X* **6,** 041015. arXiv: 1606.04856 [gr-qc] (Oct. 2016).
7. Abbott, B. P. *et al.* Upper Limits on the Rates of Binary Neutron Star and Neutron Star-Black Hole Mergers from Advanced LIGO's First Observing Run. **832,** L21. arXiv: 1607.07456 [astro-ph.HE] (Dec. 2016).
8. Abbott, B. P. *et al.* The Rate of Binary Black Hole Mergers Inferred from Advanced LIGO Observations Surrounding GW150914. **833,** L1. arXiv: 1602.03842 [astro-ph.HE] (Dec. 2016).
9. GarcıA-Berro, E., Aznar-SiguáN, G. & LoréN-Aguilar, P. *White dwarf dynamical interactions* in *Fourteenth Marcel Grossmann Meeting - MG14* (Jan. 2018), 1897–1902.
10. Kremer, K., Lu, W., Rodriguez, C. L., Lachat, M. & Rasio, F. A. Tidal Disruptions of Stars by Black Hole Remnants in Dense Star Clusters. **881,** 75. arXiv: 1904.06353 [astro-ph.HE] (Aug. 2019).
11. Carroll, B. W. & Ostlie, D. A. *An Introduction to Modern Astrophysics* (Cambridge University Press, New York City, New York, 2017).

12. Shapiro, S. L. & Teukolsky, S. A. *Black Holes, White Dwarfs, and Neutron Stars: The Physics of Compact Objects* (John Wiley & Sons, Inc., 1983).

13. Bludman, S. & Kennedy, D. C. Scaling Symmetry and Integrable Spherical Hydrostatics. *J. Mod. Phys.* **4,** 486–494. arXiv: 1112.4223 [math-ph] (2013).

14. Werner, K., Hammer, N. J., Nagel, T., Rauch, T. & Dreizler, S. in *14th European Workshop on White Dwarfs, ASP Conference Series, Vol. 334 Proceedings of a meeting held at Kiel, July 19-23, 2004. Edited by D. Koester and S. Moehler. San Francisco: Astronomical Society of the Pacific, 2005, p.165* (eds Koester, D. & Moehler, S.) 165 (2005).

15. Ciardullo, R. *The Equation of State* June 2017. http://personal.psu.edu/rbc3/A534/lec7.pdf.

16. Nouh, M. I. *et al.* White Dwarf Stars as Polytropic Gas Spheres. *Astrophysics* **59,** 540–547 (Dec. 2016).

17. Bransden, B. H. & Joachain, C. J. *Introduction to Quantum Mechanics* (Longman Group UK Limited, Harlow Essex, England, 1989).

18. Liu, J. *et al.* A wide star-black-hole binary system from radial-velocity measurements. **575,** 618–621 (Nov. 2019).

19. Dolan, J. F. How to Find a Stellar Black Hole. *Science* **292,** 1079–1080. ISSN: 0036-8075. eprint: https://science.sciencemag.org/content/292/5519/1079. https://science.sciencemag.org/content/292/5519/1079 (2001).

20. Monaghan, J. J. Smoothed particle hydrodynamics. **30,** 543–574 (Jan. 1992).

21. Gaburov, E., Lombardi James C., J. & Portegies Zwart, S. On the onset of runaway stellar collisions in dense star clusters - II. Hydrodynamics of three-body interactions. **402,** 105–126. arXiv: 0904.0997 [astro-ph.SR] (Feb. 2010).

22. Wang, B. Mass-accreting white dwarfs and type Ia supernovae. *Research in Astronomy and Astrophysics* **18,** 049. arXiv: 1801.04031 [astro-ph.SR] (May 2018).

23. Press, W. H., Teukolsky, S. A., Vetterling, W. T. & Flannery, B. P. *Numerical Recipes in Fortran77: The Art of Scientific Computing* 2nd ed. (Cambridge University Press, New York City, New York, 1992).